한국동력기계공학회지 제17권 제5호 pp. 78-85 2013년 10월 (ISSN 1226-7813)
Journal of the Korean Society for Power System Engineering, Vol. 17, No. 5, pp. 78-85, October 2013
Research paper

Study on the heat transfer properties of raw and ground graphene coating on the copper plate

Sin-il Lee*, Md. R. Tanshen*† , Kwang-sung Lee*, Myekhlai Munkhshur*, Hyo-min Jeong* and Han-shik Chung*

(received 21 August 2013, revised 07 October 2013, accepted 07 October 2013)

Abstract : A high thermal conductivity material, namely graphene is treated by planetary ball milling machine to transport the heat by increasing the temperature. Experiments were performed to assess the heat transfer enhancement benefits of coating the bottom wall of copper substrate with graphene. It is well known that the graphene is unable to disperse into base fluid without any treatment, which is due to the several reasons such as attachment of hydrophobic surface, agglomeration and impurity. To further improve the dispersibility and thermal characteristics, planetary ball milling approach is used to grind the raw samples at optimized condition. The results are examined by transmission electron microscopy, x-ray diffraction, Raman spectrometer, UV-spectrometer, thermal conductivity and thermal imager. Thermal conductivity measurements of structures are taken to support the explanation of heat transfer properties of different samples. As a result, it is found that the planetary ball milling approach is effective for improvement of both the dispersion and heat carriers of carbon based material. Indeed, the heat transfer of the ground graphene coated substrate was higher than that of the copper substrate with raw graphene.

Key Words : Graphene, Heat Transfer, Copper Substrate, Thermal Conductivity

1. Introduction

Managing high thermal loads has become very critical in the rapid developed infrastructure, industrial, transportation, defense, space sectors. Several cooling technologies have been researched recently[1~2]. Conventional heat transfer techniques that rely on fluids like water[3], ethylene glycol[4], and mineral oils[5] continue to be popular due to its simple nature. Conventional heat transfer systems used in applications like petrochemical, refining, and power generation are rather large and involve significant amount of heat transfer fluids. In certain cooling applications, small heat transfer systems are required. These applications have a critical relationship between size of a mechanical system and the cost associated with manufacturing and operation. Improvements could be made in the existing heat transfer systems by enhancing the performance of heat transfer fluids resulting in lesser heat exchanger surface area, lower capital costs, and higher energy efficiencies. In this pursuit, numerous techniques to enhance the thermal performance of heat transfer fluids have

*Sin-il Lee, *† Riyad Tanshen(corresponding author), *Kwangsung Lee, *Myekhlai Munkhshur, *Hyo-Min Jeong, Han-Shik Chung : Department of Energy and Mechanical Engineering, Institute of Marine Industry, Gyeongsang National University, E-mail : hmjeong@gnu.ac.kr Tel: 055-646-4766

been investigated. One of the methods used is to add nanoparticles of highly thermally conductive materials like carbon, metal, metal oxides into heat transfer fluids to improve the overall thermal conductivity. Nanoparticles could be either spherical, cylindrical or planar in shape. In the nanofluids research, the most available shape of nanoparticle in the market is spherical such as Al, TiO2, Al2O3, Cu and CuO. Carbon nanoparticles of cylindrical form are called carbon nanotubes (CNT)[6~7]. One type of carbon nanotube is called multi-walled carbon nanotubes because they have multiple concentric tubes in a single configuration. Of its planar forms are referred as a Graphene which has several layers with nanosized.

Novoselov and Geim have discovered the Noble prize winning Graphene with a single-layer hexagonal lattice of carbon atoms and two dimensional (2D) material in 2004[11], it has been utilized to enhance heat transfer of the base fluids. In addition, Graphene is noticed to have several unique physicochemical properties, such as high surface area, excellent thermal conductivity, strong mechanical strength, good electric conductivity and very high electron mobility (~2/V·s) [19, 20], and it has drawn much attention for its engineering applications [12, 13]. However, there are two main issues for their applications in structural materials. First, entanglement of GN occurs due to their planar and winding shapes, as well as due to Van der Waals forces between them. Second, weak interfacial interactions between the GNs and the matrix occur due to the hydrophobic surfaces of the GNs. These phenomena degrade the material properties of GNs reinforced composites. In order to compensate for these issues, many studies have been conducted with various dispersion methods, such as ultrasonication[8],chemical functionalization[9], and mechanical grinding[10].

The aim of the present study was to improve the heat transfer properties of Graphene by using ball milling approach that have been deposited on the copper substrate by using etching method. To upgrade the overall quality of these materials, the planetary ball milling machine has been utilized to grind the carbon based materials. Moreover, we successfully enhanced the thermal conductivity of the Graphene using the optimized grinding condition in the planetary ball mill. Based on the experimental results, we discuss the possible mechanism for increasing and decreasing the heat transfer characteristics of the materials in this article.

2. Experimental setup

2.1 experimental apparatus and procedure

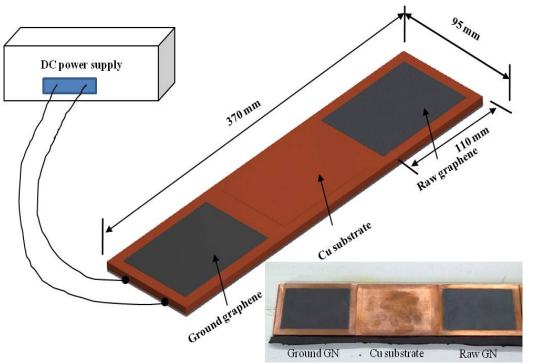

Fig. 1 Schematic diagram and real experimental picture.

The copper substrate consisting of 370 mm length and 95 mm wide is powered by plate type of heater was used in this study to compare the raw and ground graphene on the heat transfer characteristics. The thickness of the copper substrate was 5 mm. Both parts of the substrate were perfectly attached with a flat plate type of an electric heater using a thin layer of the highly thermal conductive glue. The working input power

is maintained in the ranging from 0 watt to 300 watt. Fig. 1 shown schematic diagram and real experiment picture.

2.2 preparation of nanofluids

GN (AO-2) with a specific surface area (SSA) of 100m g2and 99.9% purity (purchased from Graphene Supermarket, USA) was used as the GN source. The GN has an average thickness of 8 nm (consisting of 20-30 monolayers) and a lateral size of averaging 550 nm. Generally, theraw GNs have a hydrophobic surface[14], which is prone to aggregation and precipitation in base fluids in the absence of a dispersant/surfactant. For better dispersion, raw GNs were purified by simple method that using nitric acid (HNO3) and sulphuric acid (H2SO4) with concentration of 63% and 98% (1:3 v/v), respectively was employed. The detailed purification process of acid oxidation was previously described[10)], which was applied on carbon nanotubes. Purification was performed by ultrasonication 1510E-DTH (Branson Ultrasonic Corporation 41, USA) for 5 h to remove the impurities and to improve exterior activity. Calorimetry was performed to measure the output power and frequency of the applied ultrasonic vibration (63 W and 42 kHz, respectively).

The structure, size and purity of raw and purified GN were confirmed by Scanning electron microscopy (SEM) (JSM= 6701F JEOL) Fig. 2 shows SEM micrographs of pristine GN and ground GN. As in Fig. 2a shown, morphology of pristine GN is rough and has not good dispersibility. After grinding process ground GN surface are getting homogeneous and good dispersibility .The TEM images of pristine GN and grinding GN transmission electron microscopy (TEM) (JEM-2010 JP, JEOL), as shown in Fig. 3. As shown in Fig. 3a, it can be clearly seen that the raw GN appears densely agglomerated and in a larger planar structure. The agglomeration of the GN could have been due to the lack of hydrophilic groups and the strong π-π staking interactions on its surface. In contrast, Fig. 3b shows that the agglomeration rate of GN was slightly decreased after acid oxidation. The decreased agglomeration of the purified GN was because of the presence of hydrophilic groups (e.g., hydroxyl, epoxy, or carboxyl) on its surface.

Based on the previous work[6)], the purified GN structure was ground under wet condition at a rotation speed of 500 rpm for 1 h. In the present study, a planetary ball mill (HPM-700) (Haji Engineering, Korea) was used to grind the sample. Monosized (3.0 mm) spherical zirconia (ZrO2) balls were used as the collision medium. Grinding process was performed as following published literature[6)]. The direction of the pot rotation was set counter to that of the disk revolution.

For better dispersion, the raw and ground GNs were ultrasonically dispersed in an aqueous solution for 40 min. Ice water was repeatedly added to the ultrasonic bath during ultrasonication to prevent an increase in the temperature of the suspension. The concentration of GNs in aqueous solution was adjusted to 0.1 wt%. After that, we made paste by well dispersed GNs nanoparticles to deposit the particles on the substrate.

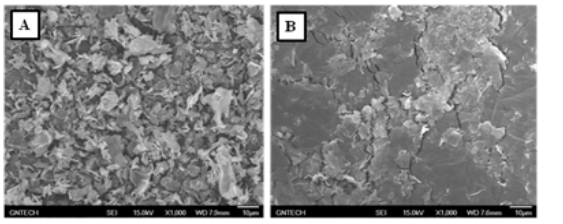

Fig. 2 SEM images of the (a) raw and (B) Ground GNs.

2.3 characterizations

The current study is compared dispersibility and

light absorption of the raw and ground structures that were dispersed in aqueous solution, and their stabilities were determined with an ultraviolet–visible (UV–vis) spectrometer (X–ma 3000 Series,) at wavelength ranging between 400–800 nm. Transmission electron microscopy (TEM) (JEM–2100F, JEOL) was used to observe the structural characterization of samples. X-ray diffraction (XRD) measurements were taken with a Bruker AXS, D8 advance powder diffractometer, using Cu Kα radiation (λ = 1.5406 Å). The samples were rotated at 10 rpm and swept from 2θ = 10^{o} through to 90^{o} using default parameters of program of the diffractometer that was equipped with Bruker AXS Diffrac PLUS software. In addition, structural changes of the processed samples were examined by Labram HR800Raman spectrometer with a 514 nm Argon ion laser. Raman spectra were recorded in the Raman shift ranging from 1200–1700−1. Thermal conductivity of the raw and ground GNs were analyzed by a thermal conductivity analyser (LAMBDA, F5 Techno-logie GmbH, Willingshausen, Germany) operating at temperatures of 15–40^{o}C in intervals of 2.5^{o}C were used in the present work. The LAMBDA system measures the thermal conductivity of fluids according to ASTMD 2717. The operation of the instrument was based on the working principles of the transient hot wire method used for nanofluids. The sample temperature was controlled by a special double-jacket heating/cooling device, which provides a homogeneous temperature distribution. Thermal imager camera (Model- FLIR E-60) has been used for taking picture. The thermal imager was completely set and tested for several times. The experimental picture was taken at every 10 minutes after the installation of the particles and substrate are heated.

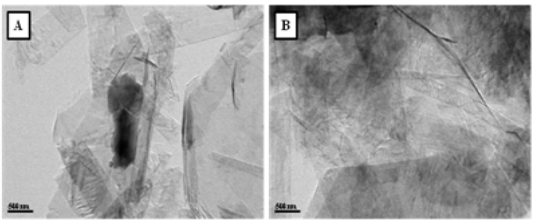

Fig. 3 TEM images of the (a) raw and (b) ground GNs.

3. Result and discussion

To study the mechanism of the dispersibility improvement, the different GNs structures were examined by XRD analysis. After the treatment processes, it is essential to keep the crystallographic structures of the materials for its next application. Figure 4 shows XRD patterns of the raw and ground GN samples. As shown in figure 4, the pronounced (0 0 2) peaks at about 26.5o and (0 0 4) peaks at about 54.6o were observed for the all GN samples and were assigned to the layer-to-layer distance (d-spacing: d = λ/2 sinθ). The interlayer spacing of raw GN was d = 3.348 Å. The interlayer spacing of ground GN was slightly increased to d = 3.355 Å, which was attributed to the impact of high–energy ball milling. In addition, the XRD pattern of the raw GN sample depicted a weak intensity (1 0 1) peak at 2θ = 44.4^{o}, (1 1 0) peak at 2θ = 77.2^{o} and (1 1 2) peak at 2θ = 83.2^{o}. These weak peaks were due to some impurities, such as soot, metal and/or amorphous carbon. Figure 4 shows that the weak peaks were not observed in the XRD patterns of ground GNs samples.

This indicates that the impurities were completely removed after the acid oxidation and grinding processes. Moreover, the XRD results ensured that the crystallographic structure of the GNs remained unchanged after the acid oxidation

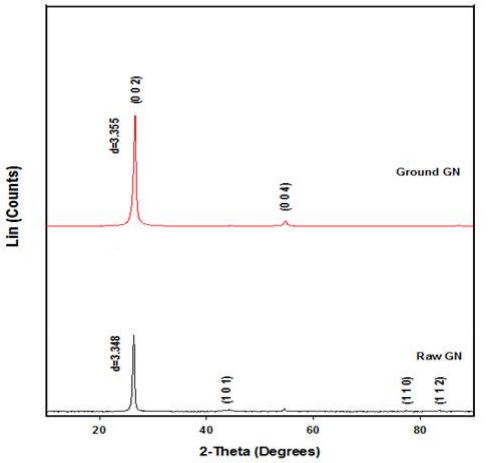

Fig. 4 XRD pattern raw and ground GNs.

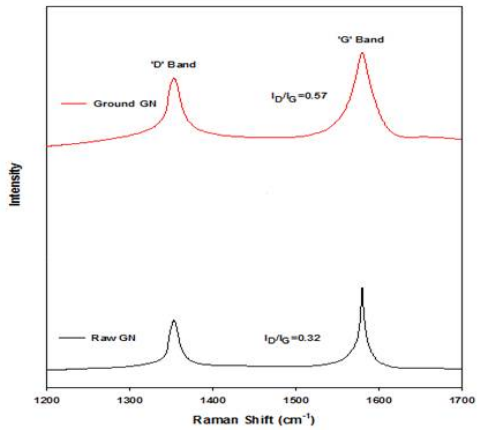

Fig. 5 Raman spectra raw and ground GNs.

and grinding processes. Raman spectroscopy is a useful tool for investigating the structural variations that occur in carbonaceous materials because it shows both the D band and the G band. Figure 5 shows the position of various peaks ofthe band and the D/G ratios for the GN structures. As shown in figure 5, the Raman spectrum of GNs samples had the characteristic G-band at a Raman shift of 1580 cm-1 and a very weak D-band at 1353 cm-1. The former was due to the vibration of sp2-bonded carbon atoms in a 2D hexagonal and the latter was caused by the vibrations of carbon atoms with dangling bonds of in-plane terminations of disordered graphite. It is worth noting that no changes in the polycrystalline characteristics of the GNs occurred. Moreover, the D/G ratio changes were generally caused by (a) an increase or decrease in the amount of amorphous carbon, (b) a higher defect density, or (c) a decrease in the crystalline size. Figure 5 shows that the D/G ratio of raw GN (0.32) increased after the grinding of GN (0.57). This increment in the D/G ratio was due to the effect of high–energy ball milling.

UV-absorption spectra were used to determine the dispersion characteristics of the suspensions[10]. It is well established that higher absorbance values generally indicate an enhanced dispersibility of particles in solution. To optimise the dispersion characteristics of the different GNs samples were studied using a UV-spectrometer. Figure 6 depicts the UV-absorption spectra at wavelengths ranging from 400 nm to 800 nm of the raw and ground GN structures that were dispersed in an anhydrous aqueous solution (0.05 wt% GN in aqueous solution). The UV light absorbance values of the raw GNs in aqueous solutions did not indicate optimal dispersion. When compared to the raw suspensions, the purified and ground GNs in aqueous solution obtained the highest UV light absorption because of their improved dispersibility. Grinding produced optimal dispersions of GNs in base. The improved dispersibility of GN in base fluid by using the ball milling method can be explained by the fact that grinding can break up large GN aggregates into smaller aggregates, and further, exfoliation can be employed to break these smaller aggregates into individual particles, which can facilitate the use of ultrasonication to disperse GNs. Individual GN particles would be well dispersed in base fluid, which is significant for practical application

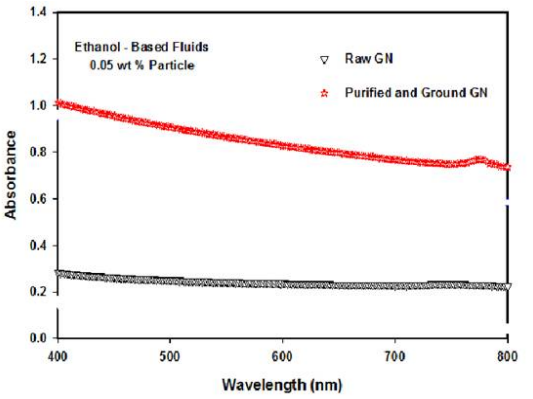

Fig. 6 UV spectophotometer of the raw and ground GNs.

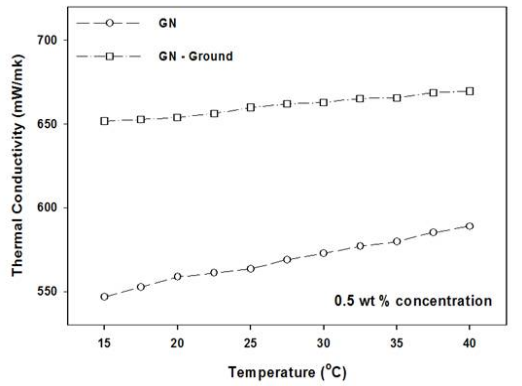

Fig. 7 Thermal conductivity of raw and ground GNs

The temperature dependence of the thermal conductivities of raw and ground GN structures are illustrated in figure 7. The thermal conductivity of the nanofluids was observed to increase linearly with temperature. One of the suggested reasons behind this phenomenon is an enhanced Brownian motion effect. Jang and Choi [15] suggested that as the temperature increases, the viscosity of the nanofluid decreases, which results in an increase in the Brownian motion of nanoparticles. It has been postulated that convection-like effects are induced by Brownian motion, which result in increased apparent thermal conductivities. Another noticeable feature is that the thermal conductivity of the ground GN was sharply higher than that of the nanofluids prepared by raw GN structure which is mainly due to the improved specific surface area and enhanced dispersion stability of GNs in aqueous solution by high energy milling method. To understand the heat transfer properties of the different GN nanoparticles, thermal imager has been used in this study, as show in figure 8a, start experiment thermal imager picture show temperature 21.8°C. As shown in figure 8b, the maximum temperature of the plate has reached until around 36.4°C for the ground GN structure which is slightly higher than that of the raw GN (around 23°C) after 120 seconds of heating. It can be seen from the figure 8c that the thermal properties images were taken after 240 seconds of the heating the plate shows slightly higher temperature than measured after 120 seconds. Moving to the figure 8d, the maximum temperature of the coated plates are constantly increased with the time.

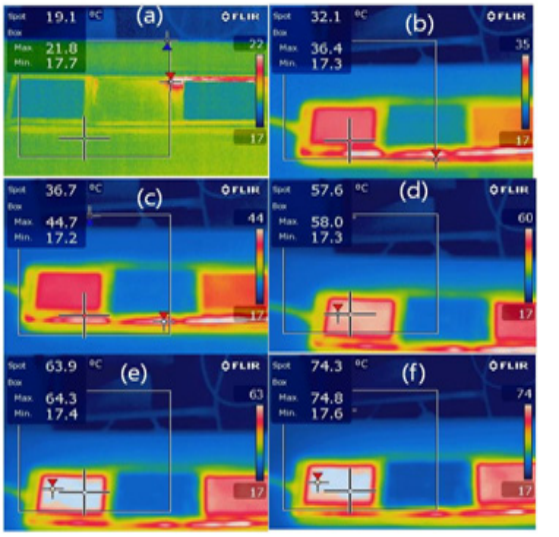

Fig. 8 The thermal properties of the raw and ground GNs.

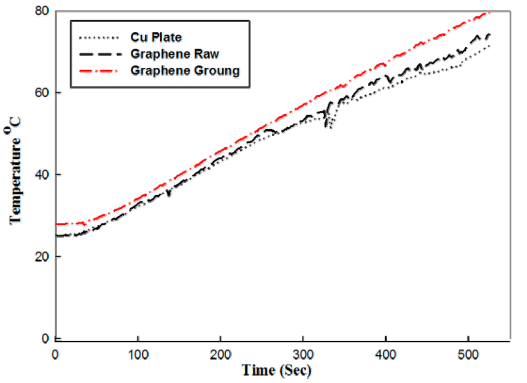

Fig. 9 Temperature distribution of raw and ground GNs.

Therefore, fig. 8e and 8f, it can be clearly observed that the thermal properties of the ground GN shows very high heat transfer characteristic than that of the copper substrate and raw GN samples. This improvement is certainly attributed to the high energy ball milling machine. Thus, thermal conductivity results are showing very good agreement with the statistical data on GN structures taken by thermal imager. To confirm the thermal imager data and thermal conductivity data, the temperature distribution of the raw and ground GNs were measured, shown in figure 9. It is clear that the temperature is gradually increased with increasing the time for both the raw and ground structures. Another noticeable feature is that the temperature distribution of the ground GN shows slightly higher temperature than that of the raw GN structures which is associated to the planetary ball milling machine, as described above.

4. Conclusion

An experimental investigation is carried out to measure the heat transfer characteristics of the raw and ground GN structures, and these data were compared to the copper substrate. As a result, we successfully improved the dispersion and thermal characteristics of the GN structures by using a planetary ball milling method. It was demonstrated that grinding can significantly enhance the dispersion stability and thermal conductivity of GN nanostructures. The enhanced dispersibility and thermal property of the GN structure can be explained by (i) increased stability, (ii) an improvement in the specific surface area and (iii) a reduction in aggregation. Grinding can break up large GN aggregates into smaller aggregates, and further, exfoliation can be employed to break these smaller aggregates into individual particles, which can facilitate the use of ultrasonication to disperse GNs. Individual GN particles would be well dispersed in base fluid, which is significant for practical applications.

Acknowledgement

This research was supported by Basic Science Research Program through the National Research Foundation of Korea (NRF) funded by the Ministry of Education, Science and Technology (NRF-2011-0009022).

References

1. Eric A. Silk, Eric L. Golliher, R. Paneer Selvam. Energy Conversion Management. 49 (2008) 453-468.
2. Theresa Pistochini, Mark Modera. Energy and Buildings. 43 (2011) 631-638.
3. B. Munkhbayar, Md. J. Nine, S. Hwang, J. Kim, K. Bae, H. Chung, H. Jeong. Chem Eng Proc. 61 (2012) 36-41.
4. Saeed Zeinali Heris. Int Comm Heat Mass Transfer. 38 (2011) 1470-1473.
5. Madhusree Kole, T.K. Dey. Int J Thermal Sci. 50 (2011) 1740-1747.
6. B. Munkhbayar, S. Hwang, J. Kim, K. Bae,

M. Ji, H. Chung, H. Jeong. Electrochimica Acta. 80 (2012) 100-107.
7. J. Ali, A. Kumar, S. Husain, M. Husain. Nanosci Nanotechnol Lett. 3 (2011) 175-180.
8. Huaqing Xie, Lifei Chen. Physics Letters A. 373 (2009) 1861-1864.
9. Liu Yang, Kai Du. Int J Refrigeration. 35 (2012) 1978-1988.
10. B. Munkhbayar. Munkhjargal Bat-Erdene, B. Ochirkhuyag, D. Sarangerel, B. Battsengel, H. Chung, H. Jeong. Materials Research Bulletin. 47 (2012) 4187-4196.
11. K. S. Novoselov, A. K. Geim, S. V. Morozov, D. Jiang, Y. Zhang, S. V. Dubonos, I. V. Grigorieva, A. A. Firsov, Science. 306 (2004) 666–669.
12. E. J. Yoo, J. Kim, E. Hosono, H. S. Zhou, T. Kudo, I. Honma, Nano Lett. 8 (2008) 2277–2282.
13. M. D. Stoller, S. Park, Z. Yanwu, J. An, R. S. Ruoff, Nano Lett. 8 (2008) 3498–3502.
14. M.Y. Yen, M.C. Hsiao, S.H. Liao, P.I. Liu, H.M. Tsai, C.C.M. Ma, N.W. Pu, M.D. Ger, Carbon. 49 (2011) 3597-3606.
15. S.P. Jang, S.U.S. Choi, Applied Physics Letters 84 (2004) 4316–4318.